$Bi_2Ca_2Sr_2Cu_3O_{10}$, whose unit cell includes an extra copper-oxygen layer. Tsuchiya *et al.* (*9*) have presented cross-sectional transmission electron microscopy results of double, triple, and quadruple copper-oxygen layers in the Bi-Ca-Sr-Cu-O systems.

None of the remaining samples, with one exception, had either a linear resistance extrapolating to zero or a pair of two superconducting transitions. To obtain superconducting transitions for the narrow diameter nonsmooth fibers, it was necessary to anneal them in air at 500°C, in contrast to the data in Fig. 6, which were obtained for an unannealed portion of the smooth fiber. This suggests that the process that forms the large oriented crystallites in the smooth fiber sections also accompanies the incorporation of adequate quantities of oxygen. The results thus indicate that an oxygen anneal lowers the resistivity and narrows the superconducting transition of the thick fibers, as well as the rough portions of thin fibers.

It is of great interest to measure the critical currents of the fibers and, following the work by Elkin *et al.* (*10*) on YBCO, improved contacts on the fibers have been made by ion milling the surface and depositing silver or gold contacts on the surface. With a pressed indium overlayer, these contacts had resistivities of 30 to 40 μohm/cm^2, but the critical current measurements are not yet complete.

We have demonstrated a capability for growing, under controlled conditions, superconducting fibers by means of the laser-heated pedestal growth technique. Under the right conditions, the growth process leads to several simultaneously occuring properties which make them ideal for study. The *a-b* planes are directed along the axis of the fiber, which we believe optimizes conduction in the axial direction. A reduced number of larger crystallites takes over during the growth of the smooth sections, which should augment the critical current. The fiber's surface morphology becomes smooth, facilitating the placement of electrical contacts. The superconducting transition consists of two distinct drops which we believe results from a phase with higher T_c.

Note added in proof: Preliminary measurements (*11*) with a pulsed current showed an excess of 60,000 A/cm^2 at 68 K.

REFERENCES AND NOTES

1. R. S. Feigelson, in *Crystal Growth of Electronic Materials*, E. Kaldis, Ed. (North-Holland, Amsterdam, 1985), pp. 127–145; in *Tunable Solid State Lasers*, P. Hammerling, A. B. Budgor, A. Pinto, Eds. (Springer, New York, 1985), pp. 129–141.
2. ——, *J. Crystal Growth* 79, 669 (1986).
3. C. A. Burrus and J. Stone, *Appl. Phys. Lett.* **26**, 318 (1974).
4. J. Bednorz and K. A. Müller, *Z. Phys. B* **64**, 189 (1986).
5. R. S. Feigelson and Y. X. Fan, paper presented at the Seventh American Conference on Crystal Growth, 12 to 17 July 1987, Monterey, CA.
6. H. Maeda, Y. Tanaka, M. Fukutomi, T. Asano, *Jpn. J. Appl. Phys.* **27**, L209 (1988).
7. See, for example: J. M. Tarascon *et al.*, *Phys. Rev. B*, in press; S. A. Sunshine *et al.*, *ibid.*, in press.
8. See, for example: R. M. Hazen *et al.*, *Phys. Rev. Lett.*, **60**, 1174 (1988); S. S. Parkin *et al.*, *ibid.*, in press; C. C. Torardi *et al.*, *Science* **240**, 631 (1988).
9. J. Tsuchiya *et al.*, in preparation.
10. J. W. Elkin, A. J. Panson, B. A. Blankenship, *Appl. Phys. Lett.* **52**, 331 (1988).
11. J. Sun, D. Fork, A. Kapitulnik *et al.*, private communications.

12. We thank R. Raymakers for making the polycrystalline starting material, C. B. Eom for assistance with the SEM photographs, J. Sun for preliminary resistivity measurements, R. Barton for useful discussions, S. Ladderman for verifying the diffraction techniques, and M. Lee for assistance in making the contacts. This work was supported by the NSF Materials Research Laboratory program through the Center for Materials Research at Stanford University.

27 April 1988; accepted 5 May 1988

Low Lake Stands in Lakes Malawi and Tanganyika, East Africa, Delineated with Multifold Seismic Data

C. A. Scholz and B. R. Rosendahl

Seismic data reveal that water level in Lake Malawi, East Africa, was 250 to 500 meters lower before about 25,000 years ago. Water levels in Lake Tanganyika at that time were more than 600 meters below the current lake level. A drier climate appears to have caused these low stands, but tectonic tilting may also have been a contributing factor in Lake Malawi. High-angle discordances associated with shallow sequence boundaries suggest that these low stands probably lasted many tens of thousands of years. Because of its basement topography, the Lake Tanganyika basin had three separate paleolakes, whereas the Lake Malawi basin had only one. The different geographies of these paleolakes may be responsible in part for the differences in the endemic fish populations in these lakes.

We have used 24-fold common depth point seismic reflection data (*1*) to delineate the boundaries of the predecessors to Lakes Malawi and Tanganyika, East Africa (Figs. 1 and 2). Mapping of paleoshorelines lying many hundreds of meters below modern lake levels is necessary for examining depositional processes in rifts, the limnology and ichthyology of African rift lakes, and the paleoclimatology of East Africa.

Lake Malawi and Lake Tanganyika occupy the southern and central parts of the western branch of the East African rift system (Fig. 1). They are among the world's deepest lakes, and both lie in a region of savannah and subtropical forest (*2–5*). Structurally, both rifts are composed of a series of linked half-grabens, which tend to have alternating directions of asymmetry along the rift axes (*6*). Modern depocenters coincide with the most subsided parts of these half-grabens. Multifold seismic data (Fig. 2, A and C) indicate that 4 km or more of sediment have accumulated in the northern basins of the Lake Malawi rift (*7*) and over 6 km of sediment fill parts of the Lake Tanganyika rift (*8, 9*).

Several seismic sequence boundaries (*10*) have been identified in the sediments beneath the main African rift lakes (*7, 8, 11, 12*). These boundaries are major breaks in the lacustrine stratigraphy and represent depositional changes that were caused by climatic, tectonic, and, in the case of the eastern rift (*13*), volcanogenic processes. The stratigraphic record of abrupt changes

Project PROBE, Department of Geology, Duke University, Durham, NC 27706.

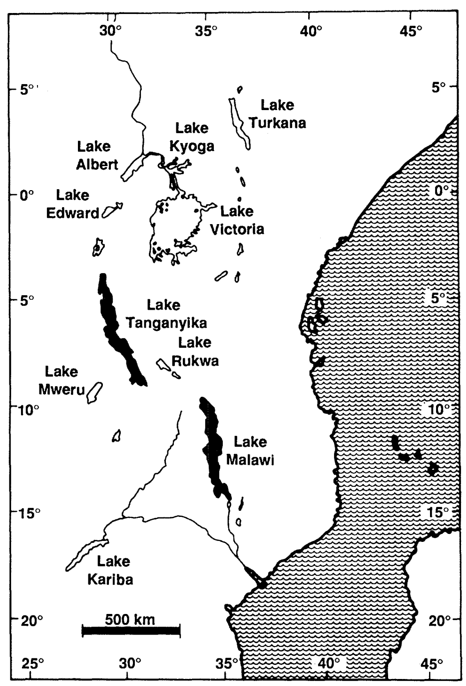

Fig. 1. The lakes of the East African rift system.

may extend back tens of millions of years in Lakes Tanganyika and Malawi (*7*, *8*). Lake levels also were highly variable in East Africa during the late Pleistocene (*12*, *14–16*), as well as during historical times (*3*, *5*, *17*).

Lakes, even large ones, are typically subject to more rapid water level changes than oceans. In rift lakes, crustal extension adds a tectonic component to lake level changes. The situation is compounded in warm, arid regions where the primary hydrologic output is by evaporation. Rapid and often large water level variations in small, high-relief drainage basins generate dynamic depositional systems. Sedimentary facies changes are common, both vertically and laterally, across lacustrine rift basins (*18*).

Ancient lacustrine environments and associated paleolake shorelines can be recognized in seismic reflection data by (i) changes in acoustic character, which are diagnostic of shallow- to deep-water facies transitions, (ii) changes in reflection termination geometries along sequence boundaries, and (iii) diagnostic external facies geometries such as wave-cut terraces and barrier systems. For example, a seismic section across the northwest part of Lake Malawi (Fig. 3) shows that a considerable part of the lower, east-dipping sequence has been truncated at the upper (that is, shallowest) sequence boundary. Truncation is a manifestation of subaerial exposure and erosion.

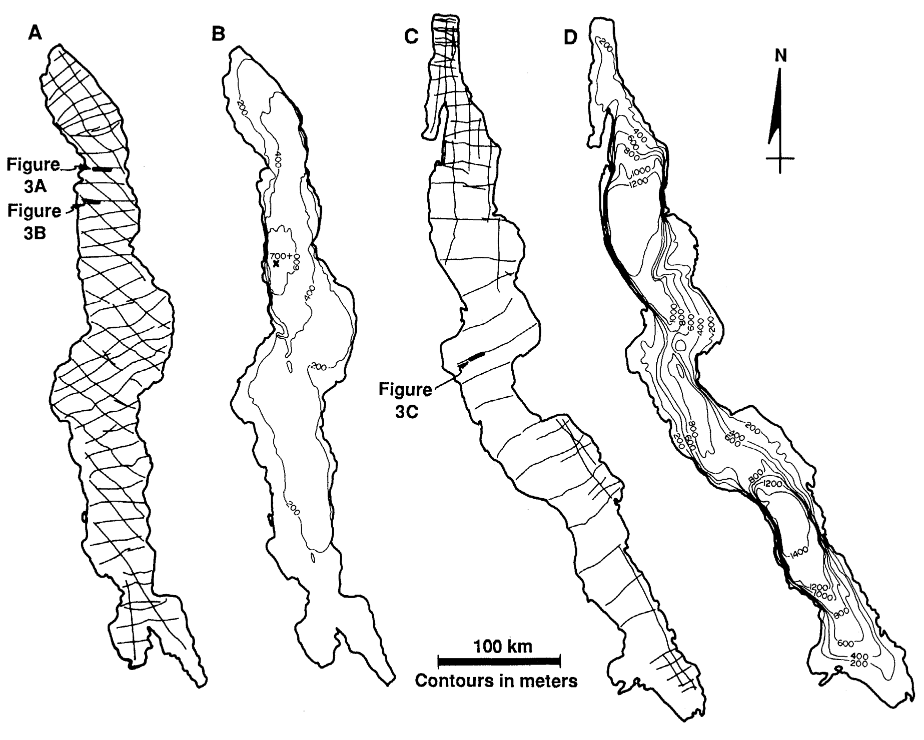

Fig. 2. (**A**) Multifold seismic coverage of Lake Malawi. (**B**) Bathymetry of Lake Malawi. (**C**) Multifold seismic coverage of Lake Tanganyika. (**D**) Bathymetry of Lake Tanganyika. Bold lines indicate locations of seismic lines in Fig. 3.

Fig. 3. (**A**) Seismic line 816 from northwestern Lake Malawi. Section from a to b shows zone of erosional truncation beneath the upper sequence boundary. Note change to a conformable relation down dip along the upper sequence boundary. Note the approximate location of the paleoshoreline for the major low lake stage discussed in text. (**B**) Seismic line 820 from west-central Lake Malawi showing continuous "open lacustrine" type acoustic facies (b to c) and wavy, semi-discontinuous "desiccated" facies above shallow basement (a to b). (**C**) Seismic line 214 from central Lake Tanganyika. Note shallow erosional surface at water depths of over 600 m. Lines displayed are 24-fold, stacked time sections with approximately 2.6:1 vertical exaggeration with respect to the water bottom. Line 214 is time-migrated.

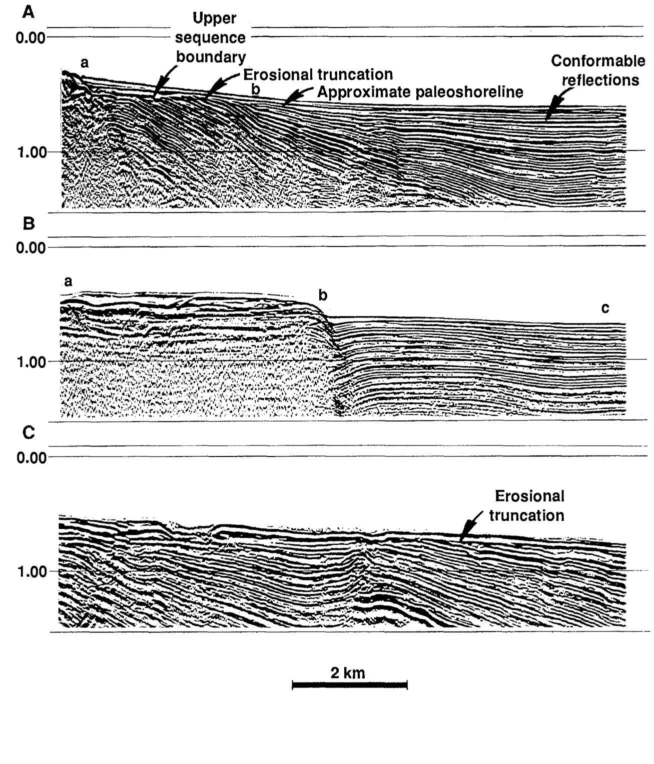

To the east of "b" on Fig. 3A, the reflection configuration along the upper sequence boundary changes to a conformable relation. Along this part of the seismic line, the thin, upper depositional sequence overlies continuous, narrow bandwidth reflections. We interpret the lower reflections as an acoustic facies indicative of continuous, open lacustrine deposits. We interpret the transition area from erosional truncation to conformable reflections as the shoreline of a previous lake level still stand, which on this profile is 400 m below the present level. In regions with steeply dipping sequence boundaries, such as on the shoaling sides of rift half-grabens, this transition is easily identified. Similar stratal relations have been recognized at comparable depths elsewhere in the northern two-thirds of Lake Malawi, as well as in several regions in Lake Tanganyika.

In west-central Lake Malawi, two distinctive acoustic facies are evident beneath the shallowest seismic sequence boundary (Fig. 3B). Toward the center of the lake (from "b" to "c" in Fig. 3B) reflections are indicative of relatively open, deep-water lacustrine sedimentation, as previously discussed. In the region from "a" to "b" the acoustic facies consists of mixed amplitude, variable frequency, wavy, and less continuous reflections. On this profile, this facies occurs at levels that are shallower than 300 m below the modern lake level. We interpret it as lacustrine deposits that were subjected to subaerial erosion and desiccation during the same late Pleistocene low stand of Lake Malawi discussed above.

The acoustic facies and reflection termination geometries that correspond to this low stand have been mapped throughout Lake Malawi (Fig. 4A). About 40 m of lacustrine sediment typically blankets the sequence boundary that is associated with the low stand. The basinward limits of erosional truncation are about 375 to 400 m below the modern lake level in the north-central part of the lake (Fig. 4A). Open lacustrine deposits occur at depths of 400 m in this area. Acoustic facies that are typical of subaerial erosion, desiccation, and nearshore conditions are recognized above the 375-m isobath (Figs. 3A and 4A). The basement topography in the Lake Malawi region makes it unlikely that this paleolake was connected to the Shire River, which currently drains Lake Malawi, or to any other outlet.

Preliminary results of ^{210}Pb sedimentation rate studies from a few Lake Malawi cores suggest that deep-water sediment has accumulated at rates of between 1 and 3 mm/year (*19*). Cryptic laminations that have been interpreted as varves suggest that sedimentation rates were about 1 mm/year (*20*). The thickness of the overlying sequence varies between a few tens of meters and about 75 m, but averages about 40 m. Assuming that the above sedimentation rates are comparable to late Pleistocene and early Holocene sedimentation rates, we estimate that this low lake stage occurred about 25,000 years ago. This is an insufficient amount of time for water level changes of such magnitude and scale to be solely attributable to tectonic subsidence. Although tectonic damming of the outlet may have caused the lake's level to rise, there is no geomorphological evidence for this. The low lake stand probably corresponds to the cooler (*21*) and presumably drier climate in the Pleistocene. The large angular discordance and large amount of erosion that are evident on many seismic lines (for example, Fig. 3A) suggest that water level in the lake was low for a long time, probably tens of thousands of years or longer. Repeated lake level drops also could have created the erosional surface; rapid changes in water level apparently occurred during the deposition of lacustrine sedimentary rocks of the Triassic rift basins in the eastern United States (*22*). However, we have been unable to resolve multiple depositional sequences, which most likely would have formed from such cyclical water level variations, from our multifold seismic data. A modern-day analog for paleo–Lake Malawi, on the basis of its size, climate, and hydrological conditions, might be modern-day Lake Turkana (Fig. 1).

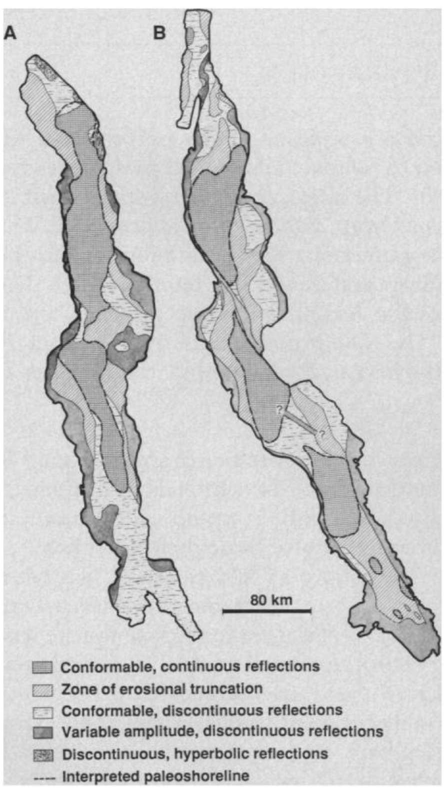

Fig. 4. (**A**) Seismic facies beneath the upper sequence boundary in Lake Malawi. Dashed line indicates approximate paleoshoreline region. Zone of conformable, highly continuous, and parallel reflections is indicative of open lacustrine conditions. Region of conformable, discontinuous reflections indicates previously desiccated lacustrine sediments. Variable amplitude, discontinuous reflections are interpreted as desiccated lacustrine sediments over shallow basement rocks. Discontinuous, hyperbolic reflections may indicate border fault talus fan deposits. (**B**) Seismic facies beneath the upper sequence boundary in Lake Tanganyika. Note interpretation of three discrete lake basins at this time. Both sequence boundaries are buried beneath an average of 40 m of sediment, as determined from multifold seismic data.

Although we infer that climatic change caused this low stand in Malawi, tectonic processes also may have had an effect. Separating climatic and tectonic controls is possible by examining the variation of mapped paleoshoreline levels from place to place. The rationale is that climatically controlled changes in water level are likely to be uniform throughout a rift lake, whereas tectonically controlled changes would almost certainly differ along a rift of Malawi's size, and may differ between adjacent half-grabens. The region of east-central Lake Malawi has a gently sloping lake floor. There is evidence here for subaerial erosion on the crests of tilted fault blocks at levels of up to 500 m below the modern lake level, compared with 375 to 400 m farther north. These estimates of paleoshoreline levels in the different structural units suggest that the lake basin has tilted southward, or perhaps pivoted around the north-central half-graben. Differential subsidence between adjacent half-grabens (*7*) or crustal doming in the Rungwe volcanic province (*23*), which lies north-northwest of the Malawi rift, could have caused this tilting.

Lake Tanganyika and Lake Malawi have similar tectonic, climatic, and physiographic settings. Stratal relations that have been inferred from multifold seismic data (*1*) (Fig. 3C) along a shallow sequence boundary in Lake Tanganyika also indicate a major low stand there. A sediment blanket in Lake Tanganyika similar in thickness and comparable in accumulation rate (*24*) to that in Lake Malawi and the large angular discordance and great amount of erosion evident on seismic lines from many areas of Lake Tanganyika suggest that this low stand was approximately contemporaneous with the one for Lake Malawi (Fig. 4B). The Lake Tanganyika low stand was also primarily related to a change in climate. The basement structure of Lake Tanganyika, particularly the occurrences of interbasinal ridges (Fig. 2D), or accommodation zones (*6*, *25*), resulted in the formation of at least three discrete basins during the low stand, in contrast to the single paleo–Lake Malawi. The ridges between these three basins probably isolated the basins from each other, creating lakes that were hydrologically, chemically, and biologically distinct. Tilting of fault blocks may have resulted in the damming of several smaller lakes, tens of square kilometers in area (Fig. 4B).

On the basis of sediment core analysis, earlier workers have postulated that the level of Lake Tanganyika also fluctuated during the late Pleistocene and Holocene (*4*, *24*, *26*, *27*). Although interpretations of the timing and amount of fluctuations of Lake Tanganyika differ in detail, there is a broad consensus that arid conditions prevailed in much of East Africa and that most lake levels were low before about 12,000 years ago (*14–16*, *27*, *28*). Paleoclimatic data in East Africa for the period before about 20,000 years ago have been obtained from only a few areas.

The Quaternary geologic history of the African great lakes likely affected evolution of their endemic fish populations (*5*, *9*). Lake Malawi supports over 200 species of cichlid fishes and Lake Tanganyika 136 species (*30*); however, Lake Malawi has only 9 families of total fishes, compared with 19 for Lake Tanganyika (*30*). The Lake Tanganyika fauna has apparently undergone a more divergent evolution than their counterparts in Lake Malawi. It has been postulated that the different hydrologies and basin morphologies of the two regions during the geologic past may have contributed to this difference in diversity (*31*). This notion is consistent with our seismic analysis. The number of ecological habitats in the three Tanganyika paleolakes presumably would have been greater than in the single basin of paleo–Lake Malawi.

REFERENCES AND NOTES

1. Multifold seismic profiling of the great lakes of East Africa has been carried out by Project PROBE of Duke University during the last 5 years. Over 3500 km of 24-fold common depth point data have been acquired on Lake Malawi (Fig. 2A) and over 2000

km on Lake Tanganyika (Fig. 2C). Single airguns or multigun arrays in the size range of 40 to 140 cubic inches (0.65 to 2.3 liters) were used for the seismic source. Incoming seismic signals were received on a 960-m long, 48-channel cable and then recorded on a Texas Instruments DFS V acquisition system aboard the Project's research vessel, *Nyanja*. TRANSAT satellites coupled to ship's velocity logs and supplemented by radar provided most navigational control. Global positioning system satellite navigation was used during about 20% of the Lake Malawi data acquisition. All Lake Malawi data have been stacked and a few lines have been migrated to date. All Lake Tanganyika dip lines have been migrated.
2. Lake Malawi is about 570 by 75 km and has a maximum depth of about 700 m (Fig. 2B). The lake is permanently anoxic below depths of about 200 m (*3*). Lake Tanganyika is about 650 by 70 km and has a maximum depth of about 1500 m (Fig. 2D). It is permanently anoxic below depths of about 150 m (*4*). Both lakes currently have outlets, although both have been closed in historical times (*5*).
3. D. H. Eccles, *Limnol. Oceanogr.* **19**, 730 (1974).
4. E. T. Degens, R. P. Von Herzen, H. K. Wong, *Naturwissenschaften* **58**, 229 (1971).
5. L. C. Beadle, *The Inland Waters of Tropical Africa* (Longman, London, ed. 2, 1981).
6. B. R. Rosendahl, *Annu. Rev. Earth Planet. Sci.* **15**, 445 (1987); C. J. Ebinger, B. R. Rosendahl, D. J. Reynolds, *Tectonophysics* **141**, 215 (1987).
7. T. Specht and B. R. Rosendahl, *J. Afr. Earth Sci.*, in press; J. Flannery, thesis, Duke University (1988). Some of the section imaged by these reflection seismic data may be of Cretaceous or Permo-Triassic (Karroo) age, although none of this section has been drilled. Preliminary velocity analyses show low values (<3500 m/s) for most of the stratigraphic section, which suggests that it is probably Cenozoic in age (C. A. Scholz, unpublished data).
8. C. F. Burgess *et al.*, in *Rifting and the Opening of the Atlantic Ocean*, W. Manspeizer, Ed. (Elsevier, Amsterdam, in press).
9. B. R. Rosendahl, J. W. Versfelt, C. A. Scholz, L. D. Woods, Eds., *Seismic Atlas of Lake Tanganyika* (Project PROBE, Duke University, Durham, NC, 1988). The Lake Tanganyika rift sediments also have never been drilled. The thickest section of sediment in this rift shows no major depositional hiatus in the deepest parts of the basin. We interpret these rift sediments to be Cenozoic in age.
10. Sequence boundaries are the unconformities and their correlative conformities that define depositional sequences. A review of the concepts of sequence stratigraphy is presented in C. E. Payton, Ed., *Am. Assoc. Pet. Geol. Mem. 26* (1977).
11. T. J. Dunkelman, J. A. Karson, B. R. Rosendahl, *Geology* **16**, 258 (1988); T. J. Dunkelman, thesis, Duke University (1986); C. J. Ebinger *et al.*, *Nature* **308**, 627 (1983).
12. T. C. Johnson, J. D. Halfman, B. R. Rosendahl, G. S. Lister, *Geol. Soc. Am. Bull.* **98**, 439 (1987).
13. A. S. Cohen *et al.*, in *Sedimentation in the African Rifts*, L. E. Frostick, R. W. Renault, I. Reid, J. J. Tiercelin, Eds. (Spec. Publ. 25, Geological Society of London, London, 1986), pp. 127–139.
14. K. W. Butzer, G. L. Isaac, J. L. Richardson, C. Washbourn-Kamau, *Nature* **175**, 1069 (1972).
15. R. L. Kendall, *Ecol. Monogr.* **39**, 121 (1969).
16. R. E. Hecky and E. T. Degens, *Woods Hole Oceanogr. Inst. Rep. 73-28* (1973).
17. M. E. Meadows, *Paleoecol. Afr.* **16**, 353 (1984).
18. B. R. Rosendahl and D. A. Livingstone, *Episodes: Q. J. Int. Union Geol. Sci.* **1983**, 14 (1983).
19. T. C. Johnson, unpublished data; K. A. Haberyan, thesis, Duke University (1988).
20. C. H. Pilskaln and T. C. Johnson, in preparation. The laminated diatomaceous muds and silts consist of couplets of white diatom-rich layers 1 mm thick and dark layers consisting of diatoms, mineral grains, and organic debris. These components are interpreted to represent seasonal flux events.
21. E. M. Van Zinderen Bakker and J. H. Mercer, *Paleogeogr. Paleoclimatol. Paleoecol.* **56**, 217 (1986).
22. P. E. Olsen, *Science* **234**, 842 (1986).
23. D. Harkin, *Geol. Surv. Tanganyika Mem. II* (1960).
24. K. A. Haberyan and R. E. Hecky, *Paleogeogr. Paleoclimatol, Paleoecol.* **61**, 169 (1987). Carbon-dated sediments from a core from southern Lake Tanganyika yielded sedimentation rates on the order of 1 mm/year. Sediment geochemistry and fossil diatom analysis indicate Lake Tanganyika was closed before about 10,000 years ago.
25. B. R. Rosendahl *et al.*, in *Sedimentation in the African Rifts*, L. E. Frostick, R. W. Renault, I. Reid, J. J. Tiercelin, Eds. (Spec. Publ. 25, Geological Society of London, London, 1986), pp. 29–43. Accommodation zones are defined as those regions where half-grabens of opposing polarity link along the strike of the rift.
26. D. A. Livingstone, *Limnol. Oceanogr.* **10**, 607 (1965); R. E. Hecky, *Pol. Arch. Hydrobiol.* **25**, 159 (1978).
27. D. A. Livingstone, *Annu. Rev. Ecol. Syst.* **6**, 249 (1975).
28. F. A. Street and A. T. Grove, *Nature* **261**, 385 (1976); A. T. Grove, *ibid.* **234**, 403 (1971).
29. G. Fryer and T. D. Iles, *The Cichlid Fishes of the Great Lakes of Africa, Their Biology and Evolution* (Oliver & Boyd, Edinburgh, 1972).
30. R. H. Lowe-McConnell, *Ecological Studies in Tropical Fish Communities* (Cambridge Univ. Press, Cambridge, 1987).
31. J. E. Brooks, *Q. Rev. Biol.* **25**, 131 (1950); E. B. Worthington, *Nature* **173**, 1064 (1954).
32. We thank the governments of Burundi, Malawi, Mozambique, Tanzania, and Zaire for permission to conduct this research. Numerous individuals at Project PROBE helped in the acquisition and processing of the data. We thank J. McGill, captain of the R.V. *Nyanja*, for his efforts during data acquisition and L. D. Woods for drafting the figures. D. A. Livingstone and T. C. Johnson reviewed earlier versions of the manuscript. We thank T. C. Johnson for permission to examine his unpublished data. This work has been supported by Agip, Amoco, Arco, Conoco, Eason, Exxon-Esso, Marathon, Mobil, Pecten, Pennzoil, Petrofina, Placid, Shell International Petroleum, Texaco, and the World Bank.

13 November 1987; accepted 22 April 1988

Amino Acid Preferences for Specific Locations at the Ends of α Helices

JANE S. RICHARDSON AND DAVID C. RICHARDSON

A definition based on α-carbon positions and a sample of 215 α helices from 45 different globular protein structures were used to tabulate amino acid preferences for 16 individual positions relative to the helix ends. The interface residue, which is half in and half out of the helix, is called the N-cap or C-cap, whichever is appropriate. The results confirm earlier observations, such as asymmetrical charge distributions in the first and last helical turn, but several new, sharp preferences are found as well. The most striking of these are a 3.5:1 preference for Asn at the N-cap position, and a preference of 2.6:1 for Pro at N-cap + 1. The C-cap position is overwhelmingly dominated by Gly, which ends 34 percent of the helices. Hydrophobic residues peak at positions N-cap + 4 and C-cap − 4.

The empirical preferences of each amino acid for the different types of secondary structure have formed a central theme of the efforts to predict three-dimensional protein structure from amino acid sequence. In almost all cases (*1–4*), those amino acid preferences have been smoothed over windows of 3 to 20 residues along the sequence, which gives statistically solid but relatively weak preference values. The only secondary structures that have been analyzed for unaveraged, single-position preferences are specific types of turns or connections; those have shown preferences as high as the 3:1 value for proline in tight turn position two (*5*), and sometimes even higher for glycine in very specifically defined connection types (*6*). Position-specific preferences have not been compiled for helices or β strands, presumably because the database was not large enough, and also because of the difficulty of settling on an unambiguous definition for placing segment ends. The database of well-determined three-dimensional protein structures is now large enough to provide statistically meaningful single-position helix preferences for all but the rarer amino acids. We use a definition of helix ends that optimizes correlation with the amino acid sequence, in order to compile those preferences here.

The sample of 215 α helices was taken from 42 proteins in the Brookhaven Data Bank (*7*), plus three revised coordinate sets: bacteriochlorophyll protein (*8*), cro repressor (*8*), and cytochrome b562 (*9*). From families of homologous proteins, only examples with low sequence similarity to each other were included. We examined the structures on an Evans and Sutherland PS 330 with a Tektronix stereo window, using the display program CHAOS (*10*), which runs entirely inside the PS 330 processor. The utility programs that calculate vectors, ribbons, H bonds, and dot surfaces for CHAOS run on a MassComp workstation under UNIX. The backbone dihedral angles ϕ and ψ were calculated by means of the DIHDRL program (*11*), modified for the UNIX MassComp. The superpositions in Fig. 2 were done with the INSIGHT pro-

Department of Biochemistry, Duke University, Durham, NC 27710.